Crack front segmentation under combined mode I- and mode III-loading

A. Eberlein

University of Paderborn, Institute of Applied Mechanics, Pohlweg 47-49, 33098 Paderborn, Germany
eberlein@fam.upb.de, http://mb.uni-paderborn.de/fam/

H. A. Richard

University of Paderborn, Institute of Applied Mechanics, Pohlweg 47-49, 33098 Paderborn, Germany
richard@fam.upb.de, http://mb.uni-paderborn.de/fam/

ABSTRACT. This article approaches the topic of crack initiation and crack growth behaviour under combined mode I- and mode III-loading conditions. Such loading combinations especially lead to a crack, which unscrew out of its initial orientation and segments into many single cracks respectively facets. This characteristic depicts the crucial difference to a crack growth under pure mode I-loading, pure in-plane shearing (mode II) as well as 2D-mixed-mode-loadings. Since this stepped fractured surfaces thus far are proved little and therefore their characterisation remains to be done, a facets quantification using some characteristic dimensions will be performed within this article. After the description of experiments for facet creation the facet's quantification using the crack profile near the initial position each facet will be analysed concerning characteristic dimensions. Finally the findings will be illustrated and discussed in this contribution.

KEYWORDS. 3D-mixed-mode; Facets; Fatigue; Fracture; CTSR-specimen.

INTRODUCTION

A by today unsolved and long existing research matter in fracture mechanics is the characterisation of crack initiation and growth behaviour under combined mode I- and mode III-loading. This loading combination specially leads the initial crack to twist out of its previous direction and separate at once into multiple daughter cracks, afterwards called facets. Building on the researches and findings from Sommer [1], Knauss [2] as well as Pons and Karma [3] within this article a quantification of facets will be presented and discussed. The purpose is to get new insights and facts about facets creation and initiation.

EXPERIMENTS FOR FACET CREATION

Creating facets experiments under mixed-mode I + III-loading were performed using the CTSR-specimen and corresponding loading device [4, 5]. A detailed explanation of the experimental procedure and CTSR-specimen's geometry follows below.

CTSR (Compact Tension Shear Rotation) -specimen

Referring to the AFM-specimen a new specimen, so-called CTSR-specimen (Fig. 1) has been developed [4]. Relevant specimen's dimensions are listed in the chart on the right hand side of Fig. 1. Hereby the specimen thickness t is a compromise between a thick specimen with a high torsional stiffness and high testing load levels. The appropriate loading device is shown in Fig. 2. In combination with the new specimen this loading device enables any combination of mixed-mode-loading including pure mode I-, pure mode II- and pure mode III-loading. A detailed explanation and illustration of adjusting the mixed-mode-loading can be found in [4, 5, 6].
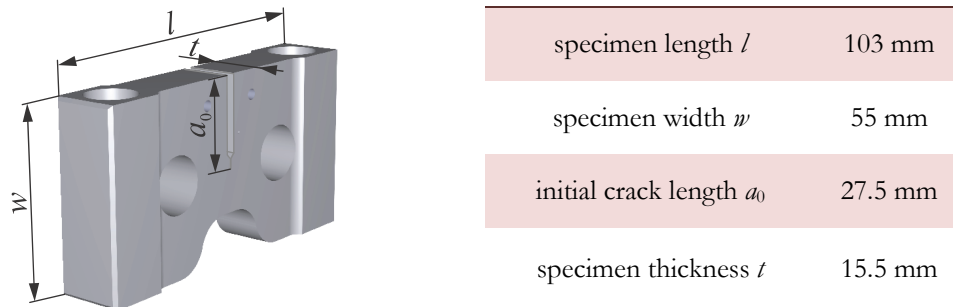

specimen length l	103 mm
specimen width w	55 mm
initial crack length a_0	27.5 mm
specimen thickness t	15.5 mm

Figure 1: CTSR-specimen with characteristic dimensions.

Experimental Procedure under combined Mode I-Mode III-loading

For the creation of facets crack growth experiments with changing loading directions were performed. After a crack growth of a crack length a = 3.5 mm under mode I-loading condition with a constant cyclic comparative stress intensity factor ΔK_V the loading direction by turning the loading device and rotating the specimen was changed into mixed-mode I + III-loading with $\Delta K_I \neq 0$ and $\Delta K_{III} \neq 0$ (Fig. 2).
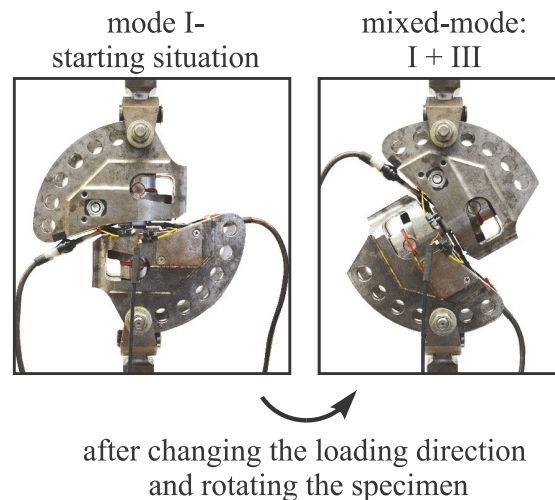
mode I-
starting situation

mixed-mode:
I + III

after changing the loading direction
and rotating the specimen

Figure 2: Mixed-mode I + III-loading by shifting the loading device.

Then the tests started again under constant cyclic load range ΔF set so, that the cyclic comparative stress intensity factor ΔK_V before and after the loading direction was identically.

Crack length-Cycle Curves and Fractured Surfaces

Typical *a-N*-curves resulting from such experiments with changing loading directions are shown in Fig. 3. The mixed-mode I + III-loading was adjusted by varying both loading angles a and β. A crack length a of 3.5 mm under mode I-loading, due to that high cyclic stress intensity factor $\Delta K_V = \Delta K_I$, is reached after ca. N = 70,000 cycles. Afterwards changing the loading direction the crack growth delays. Significant crack growth retardations were noticed by stress intensity factor ratios $1 < K_{III}/K_I < \infty$.
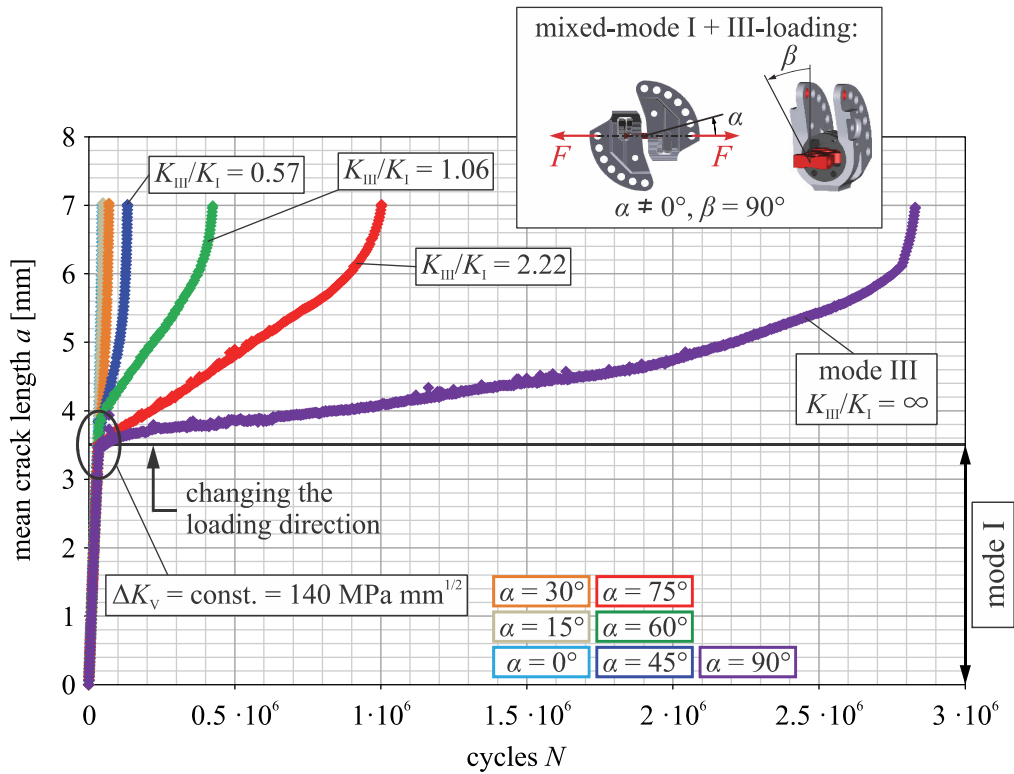
Figure 3: Crack growth retardation after changing the loading direction from mode I to mixed-mode I + III.

On the one hand the retardation effects are caused by the new crack growth direction due to mode III-loading part. Hereby the crack twists at an angle ψ_0 out of its previous orientation. Additionally the crack separates in many facets, which influence the crack growth rate too. Characteristic fractured surfaces with facet formation after changing the loading direction from mode I-loading to mixed-mode I + III-loading are pictured in Fig. 4. This row on fractured surfaces shows the facet formation depending on mode III-part on the total stress intensity factor $K_{III}/(K_I + K_{III})$. The figures indicate that facet formation begins at a specific mode III-part on the total stress intensity factor of $K_{III}/(K_I + K_{III}) = 0.37$. Within this experimental research no facets were observed below that ratio. The first fractured surface on the left hand side of Fig. 4, captured by mode III-part on the total stress intensity factor of $K_{III}/(K_I + K_{III}) = 0.26$, shows that the crack continuously and smoothly without any facet initiation changes its direction. Furthermore, the crack front is still coherent. With increasing mode III-part on the mixed-mode I + III-loading the facets' shape changes clearly.
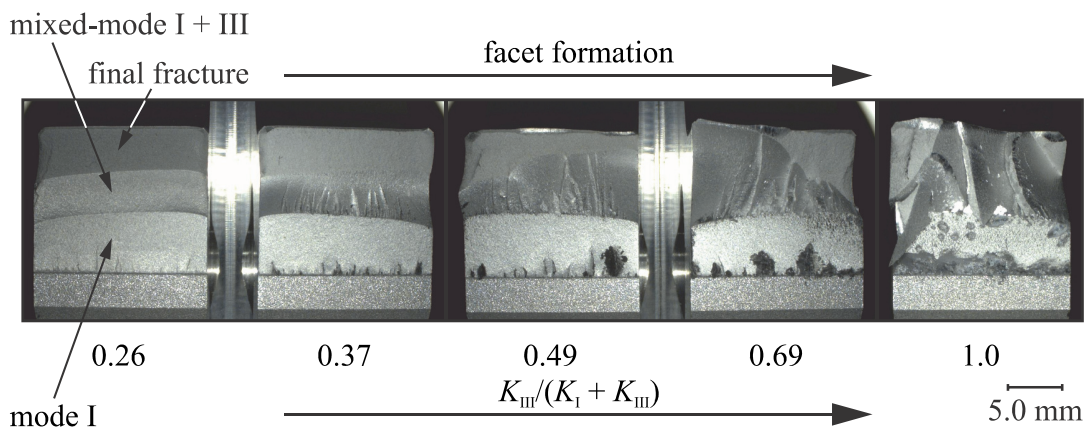

Figure 4: Facet formation with increasing mode III-part.

To get a better knowledge of such facet formation under mixed-mode I + III-loading for its consideration in existing hypotheses for crack growth prediction under 3D-mixed-mode-loadings a facet quantification was performed, which is presented and discussed in the next section.

CHARACTERIZATION OF CRACK FRONT SEGMENTATION

The first step to understand the crack growth behaviour under mode I-mode III-loading conditions is to quantify the crack front segmentation respectively the facet formation. Therefor some characteristic dimensions and angles were defined.

Definition of characteristic Dimensions

First of all, the geometry of each facet will be simplified to a circular shape. Then due to the non-planar shear stress τ_z facets initiate twisted under a facet angle ψ_F as Fig. 5 a) shows. Reflecting the work of Lin et al. [7] this facet quantification distinguishes between two facet types – ascending facets f_{as} indicated in Fig. 5 b) by red lines – and falling facets f_{fa} indicated in Fig. 5 b) by dashed lines, which finally connects the ascending facets f_{as}. Ascending facets f_{as} initiate induced by a local opening mode-loading [8] whereas falling facets f_{fa} form in a bridging region B making a connection to each f_{as} facet.
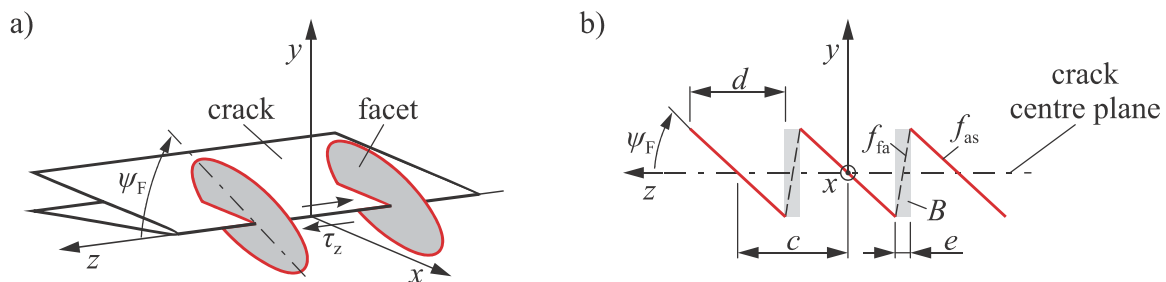

Figure 5: Definition of characteristic dimensions for facet quantification: a) Schematic facet formation at the crack front due to τ_z; b) Facet's geometry and characteristic dimensions in the y-z-plane

The f_{fa} facets are unfavourable oriented to a local opening mode-loading. Consequently, another local mechanisms, like local friction or plasticity [7], are probably responsible for their formation. So higher energies respectively loads for the creation of f_{fa} facets are required. As a conclusion such facet formation proceeds at a later crack growth stage as the initiation of f_{as} facets [3, 7]. Other characteristic dimensions for facet quantification are the projected facet length d, the facet distance c and the width e of the bridging region B (see Fig. 5 b)).

Approach for Quantification of Facet's Geometry

For facet quantification the fractured surfaces were analysed microscopically. Hereby the crack's profile was measured close to the initial notch that is after a short crack extension Δa. Fig. 6 illustrates a typical crack's profile of a mode III fractured surface. The measurement plane of crack's profile, indicated by the arrow, lies in a distance of about $\Delta a \approx 285$ μm from the wire eroded notch.

In the front view (indicated by the red arrow) the crack's profile looks as in Fig. 6 b) shown. Thereby the f_{as} facets, which were considered for the quantification, are marked in the graph. Furthermore, it is visible that in the middle of the specimen the biggest facets creates. The analysis of all f_{as} facets reveals an average projected facet length of $d = 1.23$ mm and an average distance of $c = 1.63$ mm. The biggest facet angles ψ_F exhibit the f_{as} facets $f_{as,3}$, $f_{as,4}$ and $f_{as,5}$ (see Fig. 6 b)). The angles ψ_F lie within an expected range between 42.3° and 49.3°. Starting from the middle of the specimen to the specimen borders a decreasing facet angle was noted. The reason for this is the decreasing shear stress τ_z and an increasing mode II-part by moving from the middle of the specimen to the border. Due to no pure mode III-loading condition facets near the specimen border initiate under smaller twist angles. The measurement of the bridging regions B exposed an average width e of 342 μm. Such a systematic analysis approach for facet quantification was performed for all fractured surfaces within this experimental research. In the next section the results of facet quantification are shown and discussed.
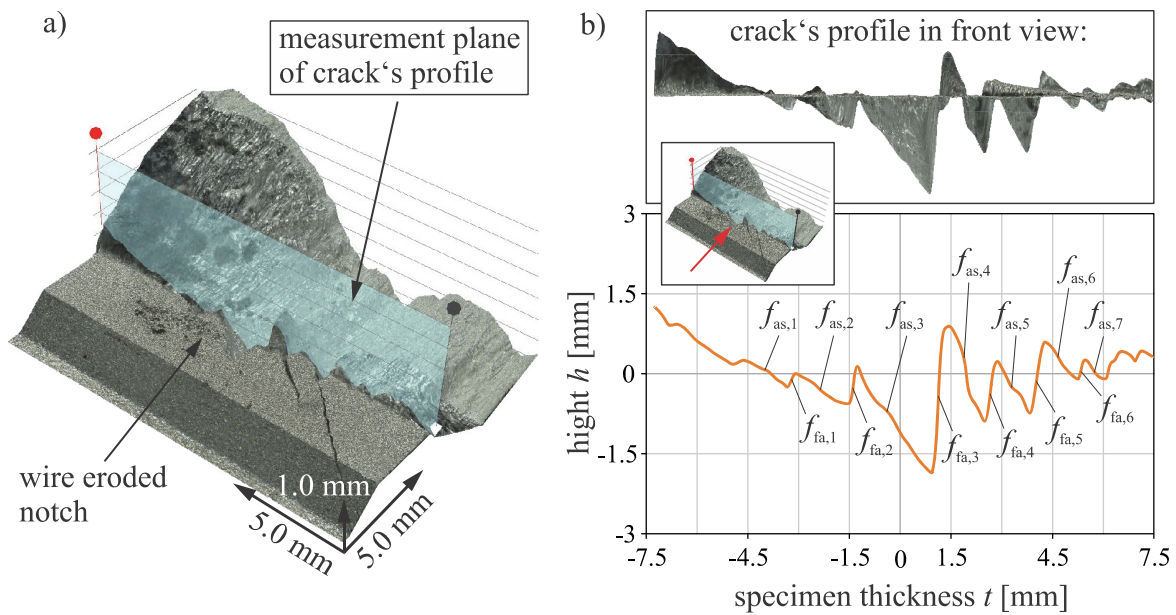
Figure 6: Analysis of facet formation: a) Fractured surface under pure mode III-loading; b) Crack's profile: measurement of each formed facet.

Results of Facet's Quantification

The results of facet's quantification are illustrated in Fig. 7. Due to the fact that within this experimental research no facets below $K_{III}/(K_I + K_{III})$ of 0.37 initiated, the number of facets in Fig. 7 a) for lower $K_{III}/(K_I + K_{III})$-ratios is zero. When facets create their quantity decreases with increasing mode III-part to an average number of five facets at pure mode III-loading. Moreover, an increasing projected facet length d and facet distance c can be detected by means of fractured surfaces (shown in Fig. 7 b)). At pure mode III-loading an average projected facet length d of 2.5 mm and an average facet distance c of 3.4 mm result.

Since the shear stress τ_z declines by moving along the specimen thickness from the middle of the specimen to the border, the conditions for pure mode III-loading are mostly given only in a limited range around the centre plane [9]. Therefore, for the measurement of the facet angles ψ_F only three facets around the centre plane of the specimen thickness are considered. Fig. 7 c) displays the results of the measured facet angles. In contrast to the hypothesis by Richard for the crack twisting angle ψ_0 the measured facet angles partially are ca. 10° smaller as the hypothesis predicts. However, the measured facet angle ψ_F for pure mode III-loading coincides very well with the hypothesis by Richard.

The determination of the facet angles respectively the crack twisting angles is principally very difficult. The measured deviations can be formed e. g. by local plastic deformations of the facets while final rupture. In addition a strong correlation between the projected facet length d, the facet distance c and the bridging width e (see Fig. 7 d)) of the bridging regions B (see Fig. 7 e)) with the measured facet angles ψ_F exist. Such a correlation between this characteristic dimensions Lin et al. found too [7]. This correlation they explain on the basis of energy's balance consideration.

The result of the bridging regions analyses is pictured in Fig. 7 d). Here the characteristic width e increases with rising mode III-part. The magnitude of the bridging width e is in comparison with the projected facet length d and the facet distance c significantly smaller and is in a direct contact with both values. At pure mode III-loading the bridging width e is almost 1 mm. Further the fractured surfaces with higher mode III-loading parts in the bridging regions B exhibit no fatigue characteristics. Instead the fractured surfaces show a classical strength failure due to cleavage fracture as well as shear fracture.

Based on this experimental knowledge of facet's creation and crack front segmentation under combined mode I-mode III-loading the next step will be an establishing of a criterion for crack growth initiation under mixed-mode I + III-loadings. In this field today only a few approaches subsist, which are subjected to many assumptions and restrictions [7, 10, 11, 12, 13].
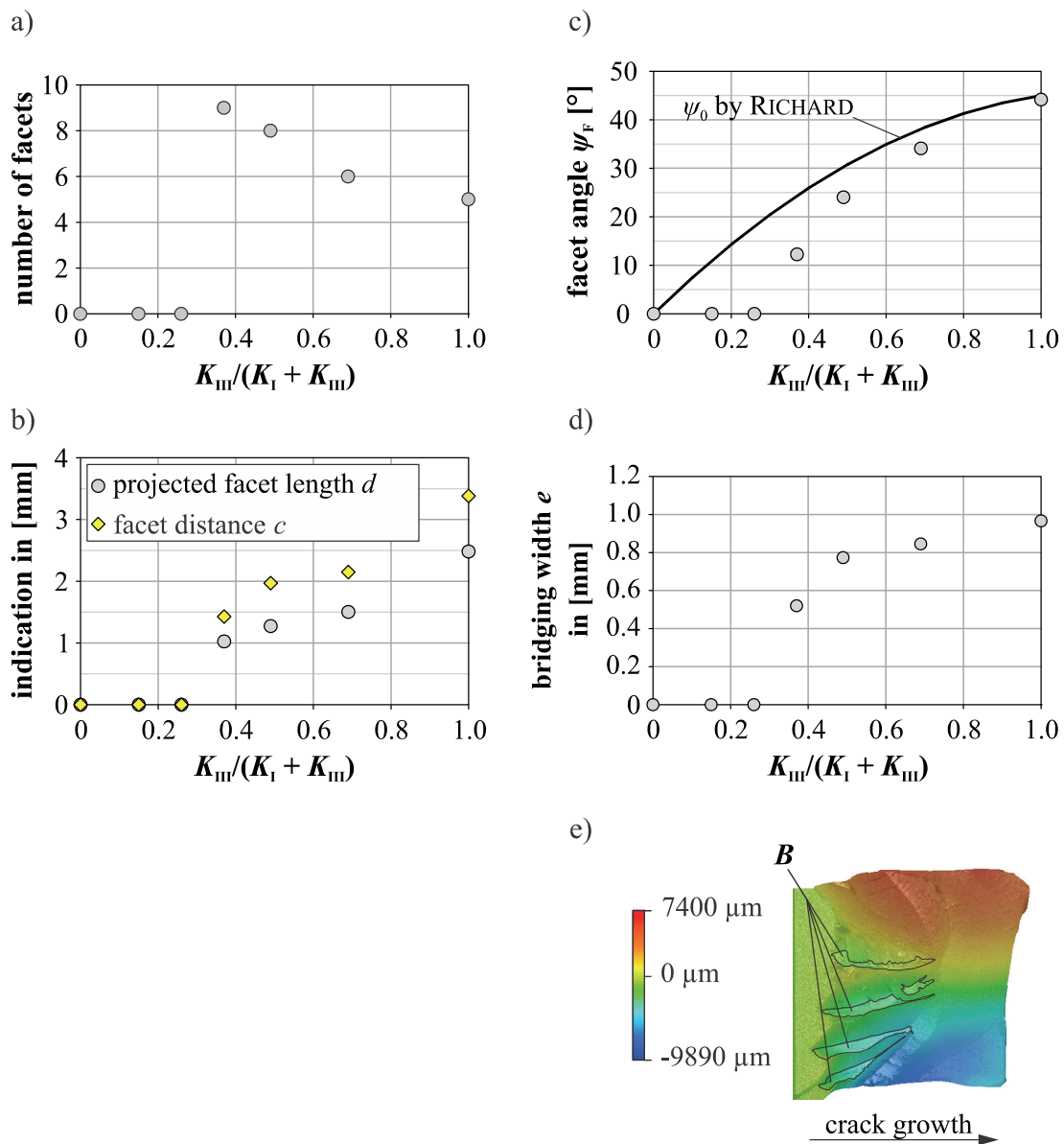
Figure 7: Overview of facets quantification's results (averages): a) Number of facets depending on mode III-part; b) Projected facet length d and facet distance c depending on mode III-part; c) Facet angle ψ_F depending on mode III-part in contrast to the crack twisting angle ψ_0 by Richard [6]; d) Bridging width e of regions B depending on mode III-part; e) Bridging regions B of a pure mode III fractured surface

REFERENCES

[1] Sommer, E., Formation of fracture 'lances' in glass, Engng. Frac. Mech., 1 (1969) 539–546.

[2] Knauss, W.G., An observation of crack propagation in anti-plane shear, Int. J. Frac., 6 (1970) 183-187.

[3] Pons, A.J., Karma, A., Helical crack-front instability in mixed-mode fracture, Nature, 464 (2010) 85-89.

[4] Schirmeisen, N.-H., Risswachstum unter 3D-Mixed-Mode-Beanspruchung, VDI-Verlag, Düsseldorf, (2012).

[5] Eberlein, A., Einfluss von Mixed-Mode-Beanspruchung auf das Ermüdungsrisswachstum in Bauteilen und Strukturen. VDI-Verlag, Düsseldorf, (2016).

[6] Richard, H.A., Schramm, B., Schirmeisen, N.-H., Cracks on Mixed-Mode loading – Theories, experiments, simulations, Int. J. Fat., 62 (2014) 93-103.

[7] Lin, B., Mear, M.E., Ravi-Chandar, K., Criterion for initiation of cracks under mixed-mode I + III loading, Int. j. Frac., 165 (2010) 175-188.

[8] Pollard, D.D., Segall, P.E., Delaney, P.T., Formation and interpretation of dilatant echelon cracks, Geol. Soc. Am. Bull., 93 (1982) 1291-1303.

[9] Kullmer, G., Richard, H.A., Wang, C., Eberlein, A., Numerische Untersuchungen zur Ermittlung der Rissablenkungs- und Rissverdrehungswinkel bei allgemeiner Mixed-Mode-Belastung, DVM-Bericht 245, Bruchmechanische Werkstoff- und Bauteilbewertung: Beanspruchungsanalyse, Prüfmethoden und Anwendungen, Deutscher Verband für Materialforschung und –prüfung e.V. Berlin (2013) 59-68.

[10] Cambonie, T., Lazarus, V., Quantification of the crack fragmentation resulting from mode I + III loading, Proc. Mater. Science 3 (2014) 1816-1821.

[11] Pham, K.H., Ravi-Chandar, K., Further examination of the criterion for crack initiation under mixed-mode I + III loading, Int. J. Frac. 189 (2014) 121-138.

[12] Leblond, J.-B., Lazarus, V., Karma, A., Multiscale cohesive zone model for propagation of segmented crack fronts in mode I + III fracture, Int. J. Frac. 191 (2015) 167-189.

[13] Ronsin, O., Caroli, C., Baumberger, T., Crack front echelon instability in mixed mode fracture of a strong nonlinear elastic solid, Europhys. Lett. 105 (2014) 34001.